Ventricular features as reliable differentiators between bvFTD and other dementias

Ana L. Manera [a,*], Mahsa Dadar [b,c], D. Louis Collins [a,1], Simon Ducharme [a,b,1], Frontotemporal Lobar Degeneration Neuroimaging Initiative (FTLDNI)[2], Alzheimer's Disease Neuroimaging Initiative (ADNI)[3]

[a] *McConnell Brain Imaging Centre, Montreal Neurological Institute, McGill University, Montreal, Quebec (QC), Canada*
[b] *Department of Psychiatry, Douglas Mental Health University Health Centre, McGill University, Montreal, Quebec (QC), Canada*
[c] *Douglas Mental Health University Institute, Verdun, QC, Canada*

ARTICLE INFO

ABSTRACT

Introduction: Lateral ventricles are reliable and sensitive indicators of brain atrophy and disease progression in behavioral variant frontotemporal dementia (bvFTD). We aimed to investigate whether an automated tool using ventricular features could improve diagnostic accuracy in bvFTD across neurodegenerative diseases.

Methods: Using 678 subjects −69 bvFTD, 38 semantic variant, 37 primary non-fluent aphasia, 218 amyloid + mild cognitive impairment, 74 amyloid + Alzheimer's Dementia and 242 normal controls- with a total of 2750 timepoints, lateral ventricles were segmented and differences in ventricular features were assessed between bvFTD, normal controls and other dementia cohorts.

Results: Ventricular antero-posterior ratio (APR) was the only feature that was significantly different and increased faster in bvFTD compared to all other cohorts. We achieved a 10-fold cross-validation accuracy of 80% (77% sensitivity, 82% specificity) in differentiating bvFTD from all other cohorts with other ventricular features (i.e., total ventricular volume and left–right lateral ventricle ratios), and 76% accuracy using only the single APR feature.

Discussion: Ventricular features, particularly the APR, might be reliable and easy-to-implement markers for bvFTD diagnosis. We have made our ventricle feature estimation and bvFTD diagnostic tool publicly available, allowing application of our model in other studies.

1. Introduction

In the absence of a unique molecular biomarker, the diagnostic certainty of the behavioral variant frontotemporal dementia (bvFTD) still relies on the convergence of clinical criteria and structural magnetic resonance imaging (MRI) or nuclear medicine imaging findings (particularly when no pathologic genetic mutation has been found). In recent work, using deformation-based morphometry (DBM), we showed

that the ventricles play a remarkable role in discriminating bvFTD from cognitively normal controls (CN) both on the voxel-wise and the anatomically defined ROI approach and ventricular expansion proved to be a sensitive indicator of disease progression (Manera et al., 2019). In this study, the lateral ventricles exhibited the most significant volumetric difference at baseline between bvFTD and CN. Furthermore, the lateral ventricles, of all the structures, showed the most significant progression of change in 1-year follow up. Furthermore, we found that the third ventricle (but not the fourth ventricle) was the second most relevant structure in terms of volumetric differences at baseline. Yet, the progression of enlargement for the third ventricle was not as significant and the magnitude of the correlation between third ventricle's annual change and annual change in disease severity was also weaker than that of the lateral ventricles. Although ventricular enlargement is not specific to bvFTD, it has been found that it has higher rates of expansion than Alzheimer's disease (AD) (Whitwell et al., 2007; Whitwell et al., 2008; Knopman et al., 2009; Tavares et al., 2019). Though shape and regional volumetric differences have been studied in AD and mild cognitive impairment (MCI) (Thompson et al., 2004; Ferrarini et al., 2006; Ferrarini et al., 2008; Tang et al., 2015), there are very few of such studies on frontotemporal dementia (Raamana et al., 2014) and, to our knowledge, there are none assessing these features particularly in the behavioral variant.

Given the sensitivity limitations of brain MRI in the early stages of FTD, there is an increasing interest in the development of automated quantitative and volumetric tools for MRI to improve diagnostic accuracy (Ducharme et al., 2020; McCarthy et al., 2018). Most of these efforts have focused on cortical atrophy measurements, however this is hard to reliably perform at the individual subject level in clinical settings, and tools based on specific cortical regions do not account for inter-subject variability in atrophy distributions. As opposed to the cortical surface, the lateral ventricles are easy to reliably segment manually or when using standard publicly available tools (Fischl, 2012; Coupé et al., 2011) and provide an estimate of the overall extent of brain atrophy across different regions, making ventricle-based features for bvFTD diagnosis a promising practical tool both in research and clinical settings. The aim of this study was to further investigate the relevance of assessing ventricle enlargement and shape features in differentiating bvFTD from other dementias, findings which are readily available from MRIs in current practice but that insufficiently used. Even when several lines of inquiry have pointed the ventricles as a good target for morphometric based aid to diagnosis, there is no method to apply this in practice. We aim to bridge this gap by developing the first tool to use ventricular features specifically for the differential diagnosis of bvFTD. We performed surface and volumetric analysis on lateral ventricles in order to find a reliable differentiator of bvFTD from AD, MCI, the language variants of frontotemporal dementia -FTD- (Semantic Variant -SV- and Progressive Nonfluent Aphasia -PNFA) and CN, with the goal of developing a clinically usable tool.

2. Materials and methods

2.1. Participants

This study included 678 subjects − 69 bvFTD, 38 SV, 37 PNFA, 218 MCI, 74 AD and 242 CN with a total of 2750 timepoints from the Alzheimer's Disease Neuroimaging Initiative (ADNI) and the Frontotemporal Lobar Degeneration Neuroimaging Initiative (FTLDNI).

The FTLDNI was funded through the National Institute of Aging and started in 2010. The primary goals of FTLDNI are to identify neuroimaging modalities and methods of analysis for tracking frontotemporal lobar degeneration and to assess the value of imaging versus other biomarkers in diagnostic roles. The project is the result of collaborative efforts at three sites in North America. For up-to-date information on participation and protocol, please visit: http://4rtni-ftldni.ini.usc.edu/. Data was accessed and downloaded through the LONI platform in

August 2018. We included all 69 bvFTD, 38 SV and 37 PNFA patients and 129 age matched CNs from the FTLDNI database who had T1-weighted (T1w) MRI scans matching with each clinical visit (Table 1). Of note, this dataset does not comprise genetic information on these subjects and, though unlikely, it is possible that some of the subjects included in the study may have a genetic mutation.

The ADNI dataset was launched in 2003 as a public–private partnership, led by Principal Investigator Michael W. Weiner, MD. The primary goal of ADNI has been to test whether serial MRI, positron emission tomography, other biological markers, and clinical and neuropsychological assessment can be combined to measure the progression of MCI and AD. ADNI was carried out with the goal of recruiting 800 adults aged from 55 to 90, and consists of 200 cognitively normal, 400 MCI, and 200 CE subjects. ADNIGO is a later study that followed ADNI participants that were in cognitively normal or early MCI stages (http://www.adcs. org/studies/imagineadni.aspx). ADNI2 study followed patients in the same categories as well as recruiting 550 new subjects (http://www. adcs.org/studies/ImagineADNI2.aspx).

In the present study, we included 74 AD amyloid β+ (defined based on the composite scores from UC Berkeley AV45 assessments provided by the ADNI with a normalized cut off threshold of 0.79), 218 MCI amyloid β + and 113 CNs from ADNI aged matched to the FTLDNI cohort (Table 1). Since a few subjects in the original datasets did not have an MRI scan available within ± 6 months from this clinical visit, these timepoints were excluded from analyses (i.e., only subjects who had T1-weighted MRI scans matching with each clinical visit were selected). All subjects included provided informed consent and the protocol was approved by the institution review board at all sites.

2.2. Neuroimaging

2.2.1. Image acquisition and preprocessing

For the FTLDNI cohort, 3.0 T MRIs were acquired at three sites (T1w MPRAGE, TR = 2 ms, TE = 3 ms, IT = 900 ms, flip angle 9°, matrix 256x240, slice thickness 1 mm, voxel size 1 mm³). Within ADNI, T1w scans from ADNI1 dataset were acquired in 3D with a gradient recalled sequence with 1.2 mm slice thickness, 160 sagittal slices, a 192 × 192 mm field of view, and a 192 × 192 scan matrix, voxel size of 1.2 × 0.9375 × 0.9375 mm, TR = 3000 ms, and TE = 3.55 ms. For ADNI2/GO datasets, T1w scans were acquired in 3D with a gradient recalled sequence with 1.2 mm slice thickness, 196 sagittal slices, covering the entire brain, a 256 × 256 mm field of view, and a 256 × 256 scan matrix, voxel size of 1 × 1 × 1.2 mm, TR = 7.2 ms, and TE = 3.0 ms.

The T1w scans of the subjects were pre-processed through our longitudinal pipeline (Aubert-Broche et al., 2013) that included image denoising (Coupe et al., 2008), intensity non-uniformity correction (Sled et al., 1998), and image intensity normalization into range (0–100) using histogram matching. Each native T1w volume from each timepoint was linearly registered first to a subject-specific template which was then registered to the ICBM152-2009c template (Collins et al., 1994). The images were visually assessed by two experienced raters to exclude cases with significant imaging artifacts (e.g., motion, incomplete field of view) or inaccurate linear/nonlinear registrations. This visual assessment was performed blind to diagnosis.

2.3. Ventricle segmentation

A previously validated patch-based label fusion technique was employed to segment the lateral ventricles (Coupé et al., 2011). The method uses expert manual segmentations as priors and estimates the label of each test subject voxel by comparing its surrounding patch against all the patches from the training library and performing a weighted label fusion using the intensity-based distances between the patch under study and the patches in the training subjects. All resulting segmentations were visually assessed, and the incomplete/inaccurate segmentations (N = 23 subjects/30 scans) were manually corrected by

Table 1

Demographic and clinical characteristics for all the cohorts. Values express Mean ± SD / Median [interquartile range]. P value level of significance: 0.05. Abbreviations: CN: cognitively normal controls; bvFTD: behavioral variant frontotemporal dementia; SV: semantic variant; PNFA: primary nonfluent aphasia; MCI: mild cognitive impairment; AD: Alzheimer's dementia; MMSE: Mini-Mental Status Examination; MoCA: Montreal Cognitive Assessment; CDR-SB: Clinical Dementia Rating-Sum of Boxes.

	NIFD				ADNI			P
	CN (N=129)	bvFTD (N=69)	SV (N=38)	PNFA (N=37)	CN (N=113)	MCI (N=218)	AD (N= 74)	
Scans	447	231	175	138	500	1037	222	
N°Scans/Subject (mean)	3.4	3.4	4.6	3.7	4.4	4.7	3	0.4
Age (y)	62±7	61±6	62±6	68±7	70±4	69±5	69±6	<0.001
Sex (male%)	56 (43%)	45 (65%)	21 (55%)	17 (46%)	64 (57%)	113 (52%)	34 (46%)	0.07
Follow-up (y)	1.3[0.6-3.4]	1[0.5-1.4]	1.2[1-16]]	1.1[0.6-1.5]	2[1.1-2.3]	2[1.1-3]	1[0.2-1.1]	<0.001
MMSE	30[29-30]	25[22-27]	26[22-28]	27[21-28]	29[29-30]	28[27-29]	24[21-25]	<0.001
MoCA	28[25-29]	19[12-23]	21[17-22]	21[10-25]	26[25-28]	23[21-26]	19[14-21]	<0.001
CDR-SB	0	6[4.5-8.5]	3.5[2.5-5.5]	2[1-3.5]	0	1.5[1-2]	4.5[3-5]	<0.001

an experienced rater. The process of segmentation QC and manual correction was performed blind to the clinical diagnosis.

2.4. Ventricular volume and shape features estimation

Using a lobe atlas of the brain delineating frontal, parietal, temporal, and occipital lobes separately in the left and right hemispheres based on the Hammers atlas (Hammers et al., 2003; Dadar et al., 2018); lateral ventricular volumes were calculated per each brain lobe and hemisphere. Using coronal coordinate y = -12 mm in the stereotaxic space (i. e., registered to the template) ventricles were divided into anterior and posterior portions. All volumes were normalized for intracranial volume and these ratios were log-transformed to achieve normal distribution. Surface and surface to volume ratio estimations where also obtained.

2.5. Reliability analysis

An important concern when establishing the utility of a metric such as APR is its test–retest reliability, i.e., the degree to which its estimates can be depended on to be precise (Dadar and Duchesne, 2020). To assess the test–retest reliability of the proposed APR measure, we processed 20 cases which had repeated MRI measurements available from the 20Repeats dataset (Dadar and Collins, 2021) using VentRA and compared the APR values estimated based on the two MRIs. Correlation coefficients and mean absolute difference (i.e. mean($\frac{|APR_1 - APR_2|}{(APR_1 + APR_2)}$)) were used to assess reliability of the proposed APR measure.

2.6. Deformation based morphometry

DBM was used to assess voxel-wise group related volumetric differences in the ventricles. Each individual scan was nonlinearly registered to the ICBM152-nonlin_sym_2009c (Manera et al., 2020) template using the Advance Normalization Tools (ANTs) diffeomorphic registration pipeline (Avants et al., 2008). The integral of the Jacobian determinant of the inverse deformation field from the non-linear transformations within the lateral ventricle was used as a measure of ventricle expansion or shrinkage. Local contractions can be interpreted as shrinkage and local expansions as enlargement of the region.

2.7. Statistical analysis

All statistical analyses were conducted using MATLAB (version R2019b). Differences in categorical variables between the cohorts were assessed using chi-square and continuous variables were assessed using one-way ANOVA or Kruskal-Wallis variance analysis depending on the distribution of the variables based on normality test. Post-hoc two-sample t-Tests were conducted to examine clinical and imaging differences at baseline. Results are expressed as mean ± standard deviation and median [interquartile range] as appropriate and P values for all the

volumetric analyses have been corrected for multiple comparisons using the Bonferroni method.

2.7.1. Voxel-wise analysis

Voxel-wise mixed effects model analysis was performed to determine the patterns of differences between each cohort and their age matched CN:

DBM ~ 1 + Cohort + Age + Sex + *(1|ID)+(1|SITE)*

where DBM denotes voxel-wise Jacobian values for subject timepoints. The variable of interest was Cohort, a categorical fixed variable contrasting each cohort versus CN. Subject ID and SITE (FTLDNI vs ADNI) were considered as categorical random effects. The models also included sex as a categorical fixed variable. The resulting maps were corrected for multiple comparisons using False Discovery Rate (FDR) controlling method, with a significance threshold of 0.05.

2.7.2. Feature analyses

Similarly, longitudinal mixed-effects models were used to assess the slope differences (with regards to changes with age) in ventricular features (anteroposterior ventricular ratio -APR- and total ventricular volume -TVV-) between bvFTD and age-matched CN as well as other dementia cohorts. In the context of this study, we refer to TVV as the total volume of the lateral ventricles, i.e., third and fourth ventricles has been not included in the analyses.

Model: feature ~ 1 + Cohort + Age + Cohort:Age + Sex + *(1|ID)+ (1|SITE)*. The variable of interest was the interaction between Cohort and Age, denoted by Cohort:Age. Age was a continuous variable varying for each follow-up timepoint. Subject ID and SITE (FTLDNI vs ADNI) were considered as categorical random effects. The models also included sex as a categorical fixed variable.

Considering the evidence in the literature showing that there might be sex-specific epidemiologic and morphometric differences in neurodegenerative disorders (Xu et al., 2000; Filon et al., 2016; Tremblay et al., 2020; Illán-Gala et al., 2021), sex was included as an additional variable to our models do account for these potential differences.

2.7.3. Diagnosis classification

To further demonstrate the diagnostic relevance of the ventricle-based features in differentiating between bvFTD and other cohorts, the baseline ventricular features were used alone and in combination with each other, age, and sex, to differentiate bvFTD from all other cohorts. A support vector machine classifier was trained on each feature set (fitcsvm function from MATLAB, with default parameters: linear kernel, Sequential Minimal Optimization) to perform the classification task, balancing the number of subjects included in each class. A 10-fold cross validation scheme was employed, and the process was repeated 100 times to obtain a robust estimate of the performance of the classifier.

2.7.4. bvFTD classification tool

The ventricle feature estimation and classification tool developed in this project (VentRa) is publicly available at: http://nist.mni.mcgill.ca/?p=2498. VentRa takes a comma separated (.csv) file providing the path for the raw T1-weighted images as well as age and sex of the subjects as input, and provides preprocessed images along with ventricle segmentations, QC files for the segmentations, as well as a .csv file including the diagnosis (based on the classifier trained on bvFTD vs the mixed group data) along with all the extracted ventricle features: i.e. total ventricle volume, ventricle volumes in each lobe and hemisphere, APR, LRTR, and LRFR ratios. To provide some examples showing the performance of the classifier, average templates of CN, bvFTD, SV, and PNFA (Dadar et al., 2020) are also included in the package, with the generated outputs. VentRa requires MATLAB and minctools, the latter available at https://github.com/BIC-MNI/minc-toolkit-v2.

3. Results

3.1. Demographics

Table 1 shows the demographic and cognitive testing performances for all the cohorts. bvFTD, SV and CN_{NIFD} subjects were younger than PNFA, CN_{ADNI} and amyloid + MCI and AD. The median follow up time in years was significantly longer for CN and MCI than AD and all the FTD related cohorts. In general, for all the cognitive/functional scores assessed CN subjects performed, as expected, significantly better than the all the other groups. There were no significant differences between bvFTD and AD cohorts in Mini-Mental Status Examination (MMSE), Montreal Cognitive Assessment (MoCA) and Clinical Dementia Rating-Sum of Boxes (CDR-SB) and they both performed significantly worse than the rest of the cohorts in all the measures. Finally, MCI subjects did not show significant differences in MMSE and MoCA scores with SV and PNFA cohorts and they had lower CDR-SB scores than AD, bvFTD and SV subjects.

3.2. Baseline ventricular volumes

Fig. 1 shows the statistically significant local differences in ventricular volumes between each cohort and CN after FDR correction, plotted on top of the average ADNI template (Atrophy specific MRI brain template for Alzheimer's disease and Mild Cognitive Impairment). Warmer colors indicate greater differences (i.e., greater degrees of ventricular enlargement). While some degree of ventricular enlargement was found for all cohorts, bvFTD showed the greatest difference in ventricular volume compared to CN; as seen in Fig. 1 the dark red anterior horns of the lateral ventricle in the bvFTD are roughly 10 time larger than CN.

The differences in lobar and total ventricular volumes between the cohorts are shown in Fig. 2. These results demonstrate an important overlap in VV between cohorts. Fig. 3 shows the left/right hemisphere ratios per lobe for the different cohorts (Panel 3A) and the APR comparison between cohorts (Panel 3B). The ventricular APR was significantly larger for bvFTD compared to all other cohorts (APR_{bvFTD} 1.4 ± 0.5, APR_{CN} 1 ± 0.2, APR_{MCI} 0.97 ± 0.2, APR_{AD} 0.92 ± 0.22, APR_{SV} 1.1 ± 0.3, APR_{PNFA} 1.2 ± 0.5; $p < 0.001$). Other relevant differences in volume are: 1) bvFTD showed significantly larger right frontal volumes than AD, MCI, SV and CN ($p < 0.001$), 2) bvFTD, AD and PNFA did not show significant differences in right parietal volume ($p = 0.08$ and $p = 0.8$, respectively), but both cohorts showed significantly larger right parietal volume than the other groups ($p < 0.001$), 3) TVV has significantly larger for all the dementia cohorts vs MCI and CN ($p < 0.001$), and 4) anterior ventricular volume did not show significant differences between bvFTD and PNFA ($p = 0.08$), yet for all of them it was significantly larger compared to the other cohorts ($p < 0.001$). Mean volumes and ratios for all the cohorts are shown in Table 1 Supplementary Material. Ventricular APR and TVV comparisons according to disease severity can also be found in Supplementary Material.

3.3. Analysis of ventricular APR differences for bvFTD severity subgroups.

Since disease duration was not available in the FTLDNI dataset we
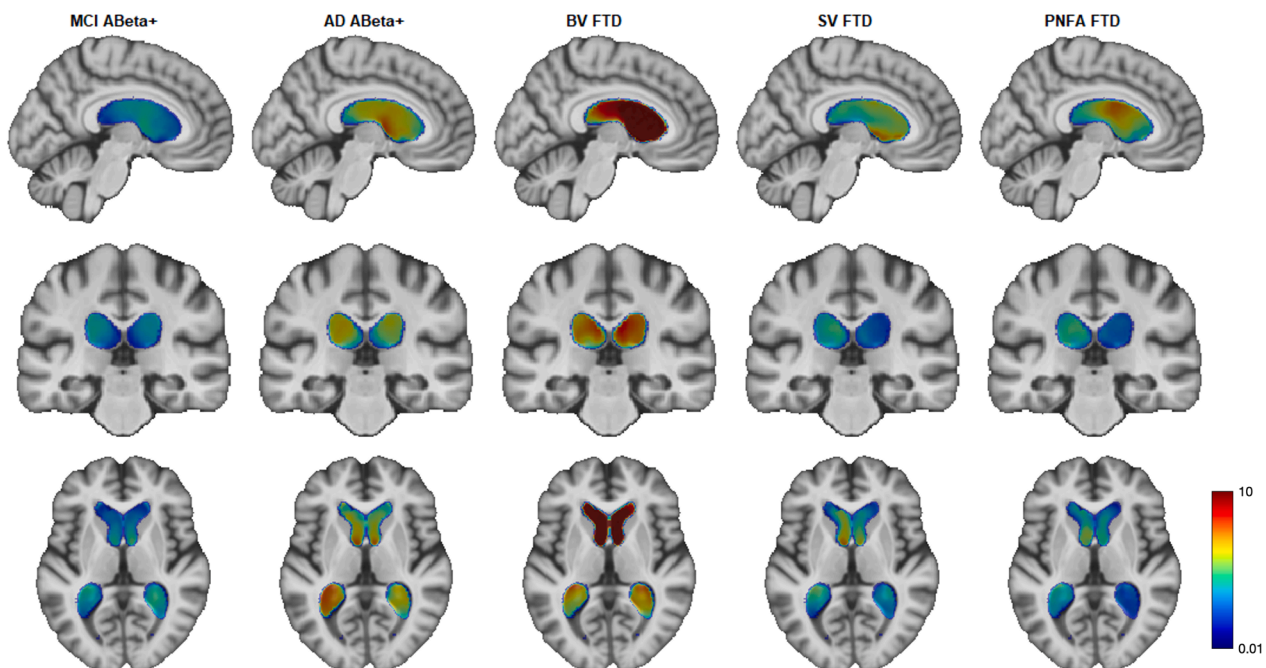

Fig. 1. Voxel-wise DBM Jacobian beta maps indicating significant ventricular differences between each cohort and age-matched controls (FDR corrected p-value < 0.05). From left to right: MCI vs CN, AD vs CN, bvFTD vs CN, PNFA vs CN and SV vs CN. Model: $DBM_{Ventricles} \sim 1 + Cohort + AGE + Sex + (1|ID) + (1|SITE)$. The figures show the significant beta values obtained for the categorical variable DX (i.e., bvFTD vs CN). Colormaps within the ventricles shows the degree of ventricle enlargement for each cohort compared to CN overlaid on the ADNI unbiased average brain template (warmer colors indicate regions with greater ventricle enlargement than regions with colder colors, varying from 1% larger to 10 times larger).
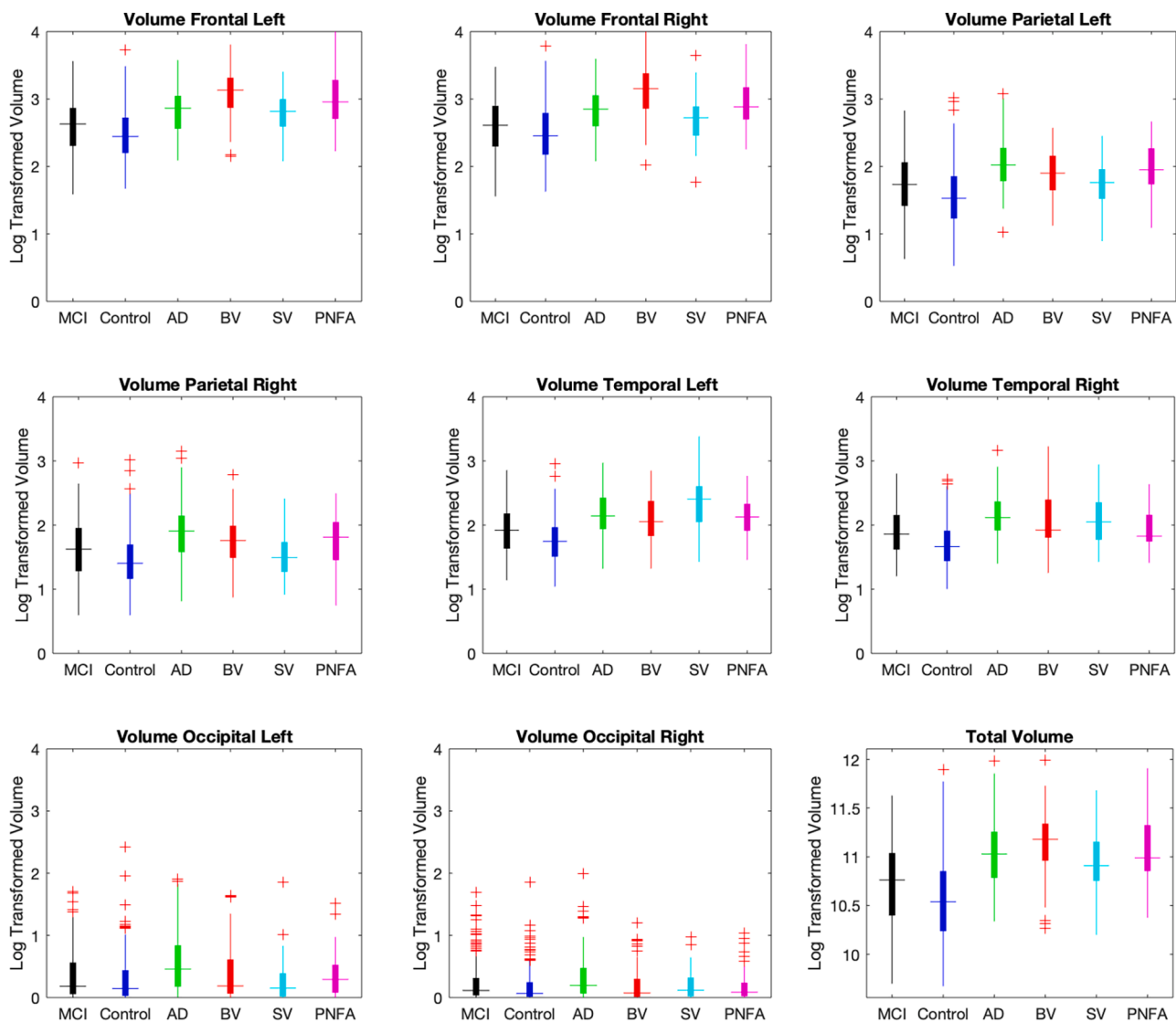
Fig. 2. Log-transformed Ventricular volume per lobe, and total ventricular volume, for different cohorts. Volumes (ml) shown are log-transformed, note that a log transformed volume of 3 corresponds to a volume of 1000 cc before log transformation. Abbreviations: MCI: mild cognitive impairment; AD: Alzheimer's disease; BV: behavioral variant; SV: semantic variant; PNFA; progressive non-fluent aphasia.

separated the bvFTD cohort into 2 subgroups according to disease severity using CDR-SB: 1) BV1 = very mild to mild bvFTD (CDR-SB $\leq$ 9 ~ CDR-Global Score $\leq$ 1), and 2) BV2 = moderate to severe bvFTD (CDR-SB > 9 ~ CDR-Global Score $\geq$ 2). Fig. S1 in the supplementary material shows that BV1 showed significant differences in APR with Controls ($p = 0.001$), MCI and AD ($p < 0.001$) but not vs the other FTD cohorts ($p = 0.32$ and $p = 0.29$ vs SV and PNFA, respectively). Whereas for BV2 significant differences in APR were found vs with all other clinical cohorts (BV2 vs Controls, $p < 0.001$; BV2 vs MCI, $p < 0.001$; BV2 vs AD, $p < 0.001$; BV2 vs SV, $p = 0.004$; BV2 vs PNFA, $p = 0.004$). Differences in TVV according to severity groups can also be found in Supplementary Materials.

3.4. Longitudinal APR change

Fig. 4 shows the slope differences (changes with age) in ventricular APR and total VV between bvFTD and age-matched CN as well as other dementia cohorts. Dotted lines indicate confidence intervals of the estimated lines. While total ventricle volume becomes larger with age in all cohorts bvFTD patients show a much faster increase in the ventricular antero-posterior ratio compared to all other cohorts ($p \leq 0.01$). This trend of increase in the ventricular antero-posterior ratio is specific to the bvFTD group; in contrast, the antero-posterior ratio decreases in CN, MCI, and AD subjects, remains relatively stable for SV subjects, and increases at a slower pace in PNFA. The SV cohort showed largest slope of increase of TVV ($P_{bvFTD vs SV} < 0.001$). While bvFTD has faster increase in TVV compared to other cohorts, this difference only statistically significant for bvFTD against CN ($P_{bvFTD vs CN} < 0.001$, $P_{bvFTD vs AD} = 0.11$, $P_{bvFTD vs MCI} = 0.8$, $P_{bvFTD vs PNFA} = 0.4$).

3.5. Classification: bvFTD vs other dementias

We further investigated the relevance of the ventricular APR in the differential diagnosis of bvFTD. This feature was used to train a classifier to differentiate bvFTD from all other cohorts both alone and in combination with TVV, LRFR, LRTR and patient characteristics (age and sex).

Using the ventricular APR alone to identify bvFTD from a mixed age-matched cohort (CN, MCI, AD, SV and PNFA) yielded a 10-fold cross-validation accuracy of 76 $\pm$ 3 % (accuracy%$\pm$std) along with 72% sensitivity and 79% specificity. Adding an additional feature such as total VV resulted in an accuracy of 80 $\pm$ 3 % (78% sensitivity and 82% specificity), while left/right temporal ratio or left/right frontal ratio did
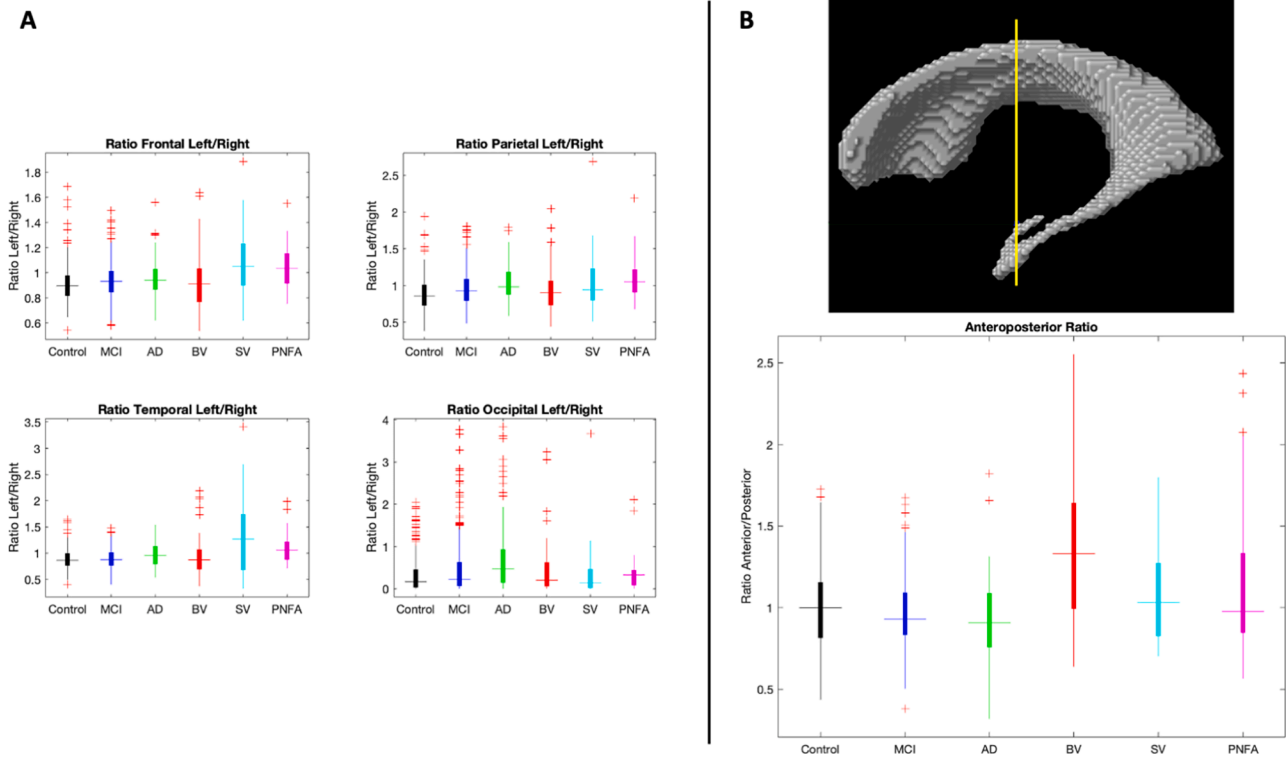
Fig. 3. Panel A: Volume left/right ratios per lobe comparison between cohorts. Panel B: Upper figure: coronal coordinate y = -12 mm for anteroposterior ratio estimation. Lower figure: Anteroposterior ratio for different cohorts (anterior ventricular volume / posterior ventricular volume). Abbreviations: MCI: mild cognitive impairment; AD: Alzheimer's disease; BV: behavioral variant; SV: semantic variant; PNFA; progressive non-fluent aphasia.
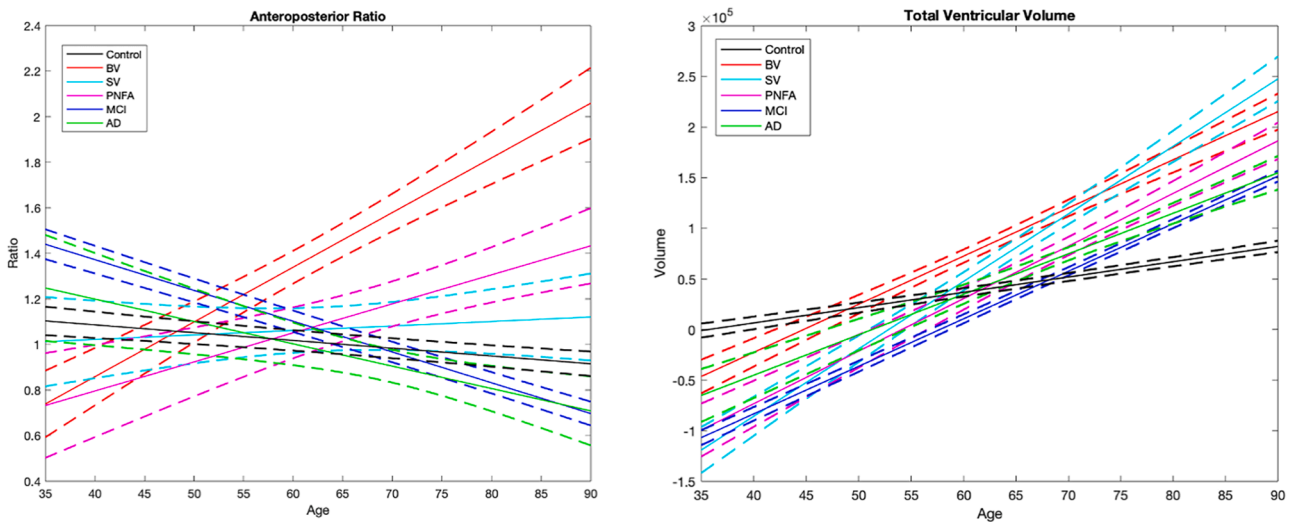

Fig. 4. Plot showing the interaction between cohort and age for total ventricular volume and antero-posterior ratio. Model: Feature ~ 1 + Cohort + Age + Cohort:Age + Sex + (1|ID)+(1|SITE). Abbreviations: MCI: mild cognitive impairment; AD: Alzheimer's disease; BV: behavioral variant; SV: semantic variant; PNFA; progressive non-fluent aphasia.

not improve global classification performances (77 ± 3 % and 75 ± 3% respectively). Using all these features together (APR + TVV + LRTR + LRFR) improved the performances in bvFTD vs all cohorts classification (accuracy 80 ± 3%, sensitivity 76% and specificity 83%).

The top accuracies against each individual cohort were 83 ± 0.02 % (81% sensitivity, 87% specificity) for bvFTD vs CN; 89 ± 2 % (87% sensitivity and 91% specificity) for bvFTD vs MCI using APR + Total VV and 83 ± 1 % (81% sensitivity and 84 % specificity) for bvFTD vs AD using APR + LRTR. The best accuracy discriminating bvFTD from SV

and PNFA were 66 ± 3 % (60% sensitivity and 72% specificity) and 71 ± 4 % (75% sensitivity and 68% specificity) respectively, using APR + TVV + LRTR + LRFR. (Fig. 5).

3.6. Reliability analysis

Running VentRA on 20 subjects with two repeated MRI scans available from the 20Repeats dataset, we extracted the APR values estimated based on each MRI. The two APR estimates were highly
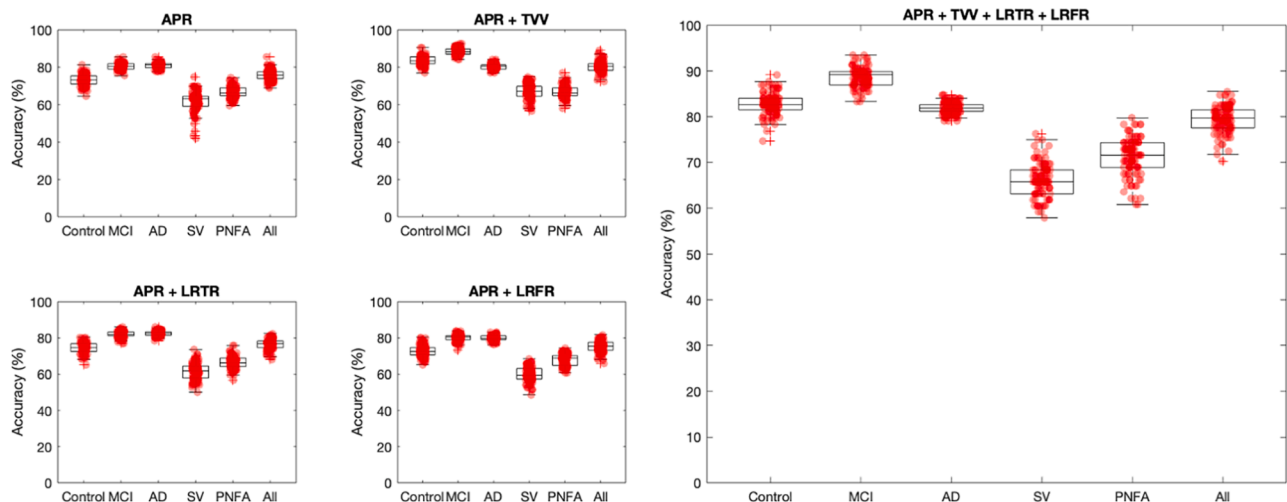
Fig. 5. Boxplots showing the mean 10-fold classification accuracy, sensitivity, and specificity with their 95% confidence intervals for bvFTD vs each individual cohort and the whole mixed dataset using age + sex + anteroposterior ventricular ratio alone and together with other volumetric ventricular features. Abbreviations: MCI: mild cognitive impairment; AD: Alzheimer's disease; BV: behavioral variant; SV: semantic variant; PNFA; progressive non-fluent aphasia. APR: anteroposterior ratio; TVV: total ventricular volume; LRTR: left/right temporal ratio; left/right frontal ratio.

correlated ($r = 0.984$, $p < 0.0001$), with mean absolute difference value of 0.034, demonstrating the robustness and reliability of the proposed measure.

4. Discussion

In this study, we investigated 1) the patterns of ventricular enlargement in bvFTD, SV, PNFA, MCI, and AD patients, and 2) the utility of ventricle-based features in differentiating bvFTD from CN, SV, PNFA, MCI, and AD. Our results showed a consistent pattern of ventricle enlargement in the bvFTD patients, particularly in the anterior parts of the frontal and temporal horns of the lateral ventricles. Temporal horns also exhibit the greatest enlargement in AD and SV compared to CN subjects.

In the cross-sectional voxel-wise DBM analysis we found that while some degree of ventricular enlargement was present in all the cohorts, bvFTD showed the greatest difference in ventricular volume compared to CN; as seen in Fig. 1 the dark red anterior horns of the lateral ventricle in the bvFTD are roughly 10 times larger compared to age-matched controls (Fig. 1). This predominantly anterior distribution of ventricular growth in bvFTD is consistent with the findings the volumetric comparisons where the anterior ventricular volume was significantly larger compared to the other cohorts except for PNFA where the difference was above the level of significance ($p = 0.08$). However, the estimation of the proposed ventricular APR resulted in statistically significant difference compared to all other groups, including PNFA. In the supplementary material, we showed that even at early stages of bvFTD (defined by CDR-SB ≤ 9 ~ CDR-SB ≤ 1), the ventricular APR is able to differentiate from controls and non-FTD cognitive disorders, making even more clinically useful.

As it might be expected, TVV has significantly larger for bvFTD, AD, SV and PNFA vs MCI and CN implying a higher degree of atrophy in dementia vs non-dementia cohorts, regardless of the regional pattern of atrophy. Finally, ventricles in bvFTD did not reveal a defined pattern of asymmetry which is consistent with the variable degree of asymmetric brain atrophy that has been described the literature; i.e., majority being symmetric with approximately 20% and 15% left and right-side predominance respectively (Gordon et al., 2016; Chapter et al., 2019; Seelaar et al., 2011; Whitwell et al., 2013).

This pattern of ventricular expansion found in the bvFTD cohort appears to be closely related to atrophy of subcortical grey matter structures as well as white matter loss. Indeed, it has been reported in

previous studies that dilation of lateral ventricles is preceded by significant atrophy of the basal ganglia, and concurrent to thinning of the corpus callosum (Kril et al., 2005). In other studies, bvFTD has shown greater subcortical atrophy at baseline and over time, which is consistent with link between subcortical atrophy and ventricular expansion (Landin-Romero et al., 2017).

Although some degree of ventricle expansion is expected with aging, the APR showed a much greater change with age than the total VV for the bvFTD group, in comparison with CN as well as with other dementia cohorts. Importantly, the significant increase in the APR is essentially a specific bvFTD feature since for other cohorts APR has minimal increase, remains stable or even decrease (i.e., other diseases impact posterior areas to a greater extent). Previously, it has been reported that FTD subjects had higher rates of expansion at all time points compared to Alzheimer's disease (Whitwell et al., 2007; Whitwell et al., 2008; Knopman et al., 2009).

The ventricular APR alone was able to differentiate bvFTD from a mixed age-matched cohort (CN, MCI, AD, SV and PNFA) with an accuracy of 76% with high specificity. Furthermore, using other ventricular features (i.e., total ventricular volume and left–right lateral ventricle ratio) we achieved 89% and 83% accuracy distinguishing bvFTD from amyloid + MCI and AD respectively, together with 66–71% accuracy for bvFTD vs other the FTD variants. Of note, the specificity and sensitivity were over 80 or 90% for all the non-FTD classifications (bvFTD vs CN, bvFTD vs amyloid + MCI and bvFTD vs amyloid + AD), which is the most clinically relevant. This performance is similar to the best performance reported in several articles that have analyzed structural MRI features (Canu et al., 2017; Möller et al., 2016; Bruun et al., 2019; Bouts et al., 2018; Zhutovsky et al., 2019). Using an anteroposterior index derived from the relation between cortical atrophy within anterior and posterior regions, Bruun et al. reported areas under the curve (AUC) values of between 0.82 and 0.85 when separating all variants frontotemporal dementia (FTD) from AD in mixed group of non-FTD dementias (AD + Lewy body disease + vascular dementia + MCI + subjective cognitive decline + others) (Bruun et al., 2019). These results are in accordance with the accuracies in the present study, supporting the diagnostic value of anteroposterior atrophy gradient. However, we used ventricular volumes and ratios as proxy of brain atrophy, making it more sensitive for detection of subcortical atrophy. The lower accuracies obtained when identifying bvFTD from SV and PNFA could be related to the well-known clinical overlap amongst all entities in the FTLD spectrum, in particular bvFTD with language variants of FTD.

To ensure that minor inaccuracies in the ventricle segmentations did not impact our results, the ventricle segmentations were strictly QCed, and the results that did not pass this QC step were manually corrected for the rest of the analyses. However, to investigate how much such inaccuracies might impact the performance of the classifier, we also repeated the classification experiments with the uncorrected segmentations, and obtained similar results (i.e., 79% accuracy, 77% sensitivity and 81% specificity for bvFTD vs all other classification). Further, the reliability analysis performed using repeated test–retest MRI scans in 20 subjects showed excellent reliability of VentRA and the proposed APR measure, further establishing the applicability potential of the proposed method.

Our results suggest that ventricular features including the ventricular APR might be useful to aid bvFTD diagnosis, particularly given that the lateral ventricles can be reliably segmented using a variety of publicly available tools such as FreeSurfer and the patch-based method used in this paper (Fischl, 2012; Coupé et al., 2011). Indeed, while combining multiple ventricular features increase the accuracy for some contrasts, the APR has the advantage of being easily measurable with good accuracy to distinguish bvFTD from all other groups.

Our study has some limitations. The FTD patients were obtained from the FTLDNI dataset, whereas the MCI and AD patients were obtained from the ADNI dataset, raising the question of whether differences in images between the two studies might have impacted the findings. The likelihood of such difference is low, given that FTLDNI and ADNI use similar scanning protocols. Further, all the image processing tools used in this study have been established and validated for use in multi-center and multi-scanner datasets (Dadar et al., 2018; Manera et al., 2021; Zeighami et al., 2015; Boucetta et al., 2016; Dadar et al., 2018), and have been designed to minimize such differences. In addition, all the voxel-wise analyses (which were most likely to be affected by such differences) compared the patient groups versus CN participants from the same study; i.e., FTLDNI bvFTD, SV, and PNFA patients were compared against FTLDNI CNs, and MCI and AD patients from ADNI were compared against ADNI CNs. The ventricle features are much less likely to be impacted by such differences, particularly for the APR, where any such differences would be cancelled out in the ratio. Finally, it is important to note that due to the limited number of FTD cohorts available, we used only cross validation in this study. In the future, it will be important to evaluate the robustness and generalizability of our results in an independent FTD cohort

The actual relevance of a biomarker aimed to distinguish behavioral vs language variants is limited for many of the cases where it is clinically evident. Yet, it could still be useful for the differential diagnosis in subjects that simultaneously fulfill clinical criteria for bvFTD and primary progressive aphasia (SV/PNFA) where brain imaging would be the hallmark. Similarly, while the value of a diagnostic algorithm to differentiate bvFTD from typical amnestic AD and MCI due to AD has limited clinical impact, such as tool has potential to facilitate the diagnosis of bvFTD in a clinical context against a broader differential diagnosis including primary psychiatric disorders. Given that primary psychiatric disorders are expected to show very modest volume lost at the most, the accuracy is expected to be close to the difference between bvFTD and CNs. This will have to be demonstrated in a mixed neuropsychiatric cohort in future work. It will also be interesting to determine the accuracy of the ratio between bvFTD and amyloid positive frontal-dysexecutive AD.

In general, the performances reported from visual radiologists' appear poorer than the classification accuracies achieved and they strongly rely on their level of experience (McCarthy et al., 2018), indicating the potential usefulness of an automated MRI-based tool for improving the diagnostic certainty of FTD. Moreover, the use of one single morphometric ratio could be more scalable than multiple semi-structured visual rating scales of atrophy that are currently recommended but inconsistently used in clinics.

5. Conclusion

Our study proposes an easy to obtain and generalizable ventricle-based feature (APR) from T1-weighted structural MRI (routinely acquired and available in the clinic) that can be used not only to differentiate bvFTD from normal subjects, but also from other FTD variants (SV and PNFA), MCI, and AD patients. In addition, we have made our ventricle feature estimation and bvFTD diagnosis tool (VentRa) publicly available, allowing application of our model in other studies. Of note, VentRa is not currently validated for clinical use. If validated in a prospective study, the proposed method has the potential to aid bvFTD diagnosis, particularly in settings where access to specialized FTD care is limited.

CRediT authorship contribution statement

Ana L. Manera: Conceptualization, Formal analysis, Data curation, Writing – original draft, Writing – review & editing. **Mahsa Dadar:** Conceptualization, Methodology, Writing – review & editing. **D. Louis Collins:** Conceptualization, Supervision, Writing – review & editing. **Simon Ducharme:** Conceptualization, Supervision, Writing – review & editing.

Declaration of Competing Interest

The authors declare that they have no known competing financial interests or personal relationships that could have appeared to influence the work reported in this paper.

grantee organization is the Northern California Institute for Research and Education, and the study is coordinated by the Alzheimer's Therapeutic Research Institute at the University of Southern California. ADNI data are disseminated by the Laboratory for Neuro Imaging at the University of Southern California.

Data collection and sharing for this project was funded by the Frontotemporal Lobar Degeneration Neuroimaging Initiative (National Institutes of Health Grant R01 AG032306). The study is coordinated through the University of California, San Francisco, Memory and Aging Center. FTLDNI data are disseminated by the Laboratory for Neuro Imaging at the University of Southern California.

Appendix A. Supplementary data

Supplementary data to this article can be found online at https://doi.org/10.1016/j.nicl.2022.102947.

References

Manera, A.L., Dadar, M., Collins, D.L., Ducharme, S., 2019. Deformation based morphometry study of longitudinal MRI changes in behavioral variant frontotemporal dementia. Neuroimage Clin. 24, 102079.

Whitwell, J.L., Jack, C.R., Parisi, J.E., Knopman, D.S., Boeve, B.F., Petersen, R.C., Ferman, T.J., Dickson, D.W., Josephs, K.A., 2007. Rates of cerebral atrophy differ in different degenerative pathologies. Brain 130 (4), 1148–1158.

Whitwell, J.L., Jack, C.R., Pankratz, V.S., Parisi, J.E., Knopman, D.S., Boeve, B.F., Petersen, R.C., Dickson, D.W., Josephs, K.A., 2008. Rates of brain atrophy over time in autopsy-proven frontotemporal dementia and Alzheimer disease. Neuroimage 39 (3), 1034–1040.

Knopman, D.S., Jack, C.R., Kramer, J.H., Boeve, B.F., Caselli, R.J., Graff-Radford, N.R., Mendez, M.F., Miller, B.L., Mercaldo, N.D., 2009. Brain and ventricular volumetric changes in frontotemporal lobar degeneration over 1 year. Neurology 72 (21), 1843–1849.

Tavares, T.P., Mitchell, D.G.V., Coleman, K., Shoesmith, C., Bartha, R., Cash, D.M., Moore, K.M., van Swieten, J., Borroni, B., Galimberti, D., Tartaglia, M.C., Rowe, J., Graff, C., Tagliavini, F., Frisoni, G., Cappa, S., Laforce, R., de Mendonça, A., Sorbi, S., Wallstrom, G., Masellis, M., Rohrer, J.D., Finger, E.C., 2019. Ventricular volume expansion in presymptomatic genetic frontotemporal dementia. Neurology 93 (18), e1699–e1706.

Thompson, P.M., Hayashi, K.M., de Zubicaray, G.I., Janke, A.L., Rose, S.E., Semple, J., Hong, M.S., Herman, D.H., Gravano, D., Doddrell, D.M., Toga, A.W., 2004. Mapping hippocampal and ventricular change in Alzheimer disease. Neuroimage 22 (4), 1754–1766.

Ferrarini, L., Palm, W.M., Olofsen, H., van Buchem, M.A., Reiber, J.H.C., Admiraal-Behloul, F., 2006. Shape differences of the brain ventricles in Alzheimer's disease. Neuroimage 32 (3), 1060–1069.

Ferrarini, L., Palm, W.M., Olofsen, H., van der Landen, R., van Buchem, M.A., Reiber, J. H.C., Admiraal-Behloul, F., 2008. Ventricular shape biomarkers for Alzheimer's disease in clinical MR images. Magn. Reson. Med. 59 (2), 260–267.

Tang, X., Holland, D., Dale, A.M., Younes, L., Miller, M.I., 2015. Baseline shape diffeomorphometry patterns of subcortical and ventricular structures in predicting conversion of mild cognitive impairment to Alzheimer's disease. J. Alzheimers Dis. 44 (2), 599–611.

Raamana, P.R., Rosen, H., Miller, B., Weiner, M.W., Wang, L., Beg, M.F., 2014. Three-class differential diagnosis among alzheimer disease, frontotemporal dementia, and controls. Front. Neurol. 5.

Ducharme, S., Dols, A., Laforce, R., Devenney, E., Kumfor, F., van den Stock, J., Dallaire-Théroux, C., Seelaar, H., Gossink, F., Vijverberg, E., Huey, E., Vandenbulcke, M., Masellis, M., Trieu, C., Onyike, C., Caramelli, P., de Souza, L.C., Santillo, A., Waldö, M.L., Landin-Romero, R., Piguet, O., Kelso, W., Eratne, D., Velakoulis, D., Ikeda, M., Perry, D., Pressman, P., Boeve, B., Vandenberghe, R., Mendez, M., Azuar, C., Levy, R., Le Ber, I., Baez, S., Lerner, A., Ellajosyula, R., Pasquier, F., Galimberti, D., Scarpini, E., van Swieten, J., Hornberger, M., Rosen, H., Hodges, J., Diehl-Schmid, J., Pijnenburg, Y., 2020. Recommendations to distinguish behavioural variant frontotemporal dementia from psychiatric disorders. Brain 143 (6), 1632–1650.

McCarthy, J., Collins, D.L., Ducharme, S., 2018. Morphometric MRI as a diagnostic biomarker of frontotemporal dementia: A systematic review to determine clinical applicability. Neuroimage Clin. 20, 685–696. https://doi.org/10.1016/j.nicl.2018.08.028 [published Online First: 2018/09/16].

Fischl, B., 2012. FreeSurfer. Neuroimage 62 (2), 774–781.

Coupé, P., Manjón, J.V., Fonov, V., Pruessner, J., Robles, M., Collins, D.L., 2011. Patch-based segmentation using expert priors: application to hippocampus and ventricle segmentation. Neuroimage 54 (2), 940–954.

Aubert-Broche, B., Fonov, V.S., García-Lorenzo, D., Mouiha, A., Guizard, N., Coupé, P., Eskildsen, S.F., Collins, D.L., 2013. A new method for structural volume analysis of longitudinal brain MRI data and its application in studying the growth trajectories of anatomical brain structures in childhood. Neuroimage 82, 393–402.

Coupe, P., Yger, P., Prima, S., Hellier, P., Kervrann, C., Barillot, C., 2008. An optimized blockwise nonlocal means denoising filter for 3-D magnetic resonance images. IEEE Trans. Med. Imaging 27 (4), 425–441.

Sled, J.G., Zijdenbos, A.P., Evans, A.C., 1998. A nonparametric method for automatic correction of intensity nonuniformity in MRI data. IEEE Trans. Med. Imaging 17 (1), 87–97. https://doi.org/10.1109/42.668698 [published Online First: 1998/06/09].

Collins, D.L., Neelin, P., Peters, T.M., Evans, A.C., 1994. Automatic 3D Intersubject Registration of MR Volumetric Data in Standardized Talairach Space: J. Comput. Assist. Tomogr. 18 (2), 192–205.

Hammers, A., Allom, R., Koepp, M.J., Free, S.L., Myers, R., Lemieux, L., Mitchell, T.N., Brooks, D.J., Duncan, J.S., 2003. Three-dimensional maximum probability atlas of the human brain, with particular reference to the temporal lobe. Hum. Brain Mapp. 19 (4), 224–247.

Dadar, M., Maranzano, J., Ducharme, S., Carmichael, O.T., Decarli, C., Collins, D.L., 2018. Validation of T1w-based segmentations of white matter hyperintensity volumes in large-scale datasets of aging. Hum. Brain Mapp. 39 (3), 1093–1107.

Dadar, M., Duchesne, S., 2020. Reliability assessment of tissue classification algorithms for multi-center and multi-scanner data. NeuroImage 217, 116928. https://doi.org/10.1016/j.neuroimage.2020.116928.

Dadar, M., Collins, D.L., 2021. BISON: Brain tissue segmentation pipeline using T1-weighted magnetic resonance images and a random forest classifier. Magn. Reson. Med. 85 (4), 1881–1894.

Manera, A.L., Dadar, M., Fonov, V., et al., 2020. CerebrA, registration and manual label correction of Mindboggle-101 atlas for MNI-ICBM152 template. Sci. Data 7 (1), 237. https://doi.org/10.1038/s41597-020-0557-9 [published Online First: 2020/07/17].

Avants, B., Epstein, C., Grossman, M., Gee, J., 2008. Symmetric diffeomorphic image registration with cross-correlation: evaluating automated labeling of elderly and neurodegenerative brain. Med. Image Anal. 12 (1), 26–41.

Xu, J., Kobayashi, S., Yamaguchi, S., et al., Gender effects on age-related changes in brain structure. AJNR Am. J. Neuroradiol., 2000;21(1):112-8. [published Online First: 2000/02/11].

Filon, J.R., Intorcia, A.J., Sue, L.I., Vazquez Arreola, E., Wilson, J., Davis, K.J., Sabbagh, M.N., Belden, C.M., Caselli, R.J., Adler, C.H., Woodruff, B.K., Rapscak, S.Z., Ahern, G.L., Burke, A.D., Jacobson, S., Shill, H.A., Driver-Dunckley, E., Chen, K., Reiman, E.M., Beach, T.G., Serrano, G.E., 2016. Gender differences in Alzheimer disease: brain atrophy, histopathology burden, and cognition. J. Neuropathol. Exp. Neurol. 75 (8), 748–754.

Tremblay, C., Abbasi, N., Zeighami, Y., Yau, Y., Dadar, M., Rahayel, S., Dagher, A., 2020. Sex effects on brain structure in de novo Parkinson's disease: a multimodal neuroimaging study. Brain 143 (10), 3052–3066.

Illán-Gala, I., Casaletto, K.B., Borrego-Écija, S., Arenaza-Urquijo, E.M., Wolf, A., Cobigo, Y., Goh, S.Y.M., Staffaroni, A.M., Alcolea, D., Fortea, J., Blesa, R., Clarimon, J., Iulita, M.F., Brugulat-Serrat, A., Lladó, A., Grinberg, L.T., Possin, K., Rankin, K.P., Kramer, J.H., Rabinovici, G.D., Boxer, A., Seeley, W.W., Sturm, V.E., Gorno-Tempini, M.L., Miller, B.L., Sánchez-Valle, R., Perry, D.C., Lleó, A., Rosen, H. J., 2021. Sex differences in the behavioral variant of frontotemporal dementia: a new window to executive and behavioral reserve. Alzheimers Dement 17 (8), 1329–1341.

Dadar M, Manera AL, Fonov VS, et al. MNI-FTD Templates: Unbiased Average Templates of Frontotemporal Dementia Variants. bioRxiv 2020.

Atrophy specific MRI brain template for Alzheimer's disease and Mild Cognitive Impairment. Alzheimer's Association International Conference; 2011 2011-07-16; France.

Gordon, E., Rohrer, J.D., Fox, N.C., 2016. Advances in neuroimaging in frontotemporal dementia. J. Neurochem. 138 (Suppl 1), 193–210. https://doi.org/10.1111/jnc.13656 [published Online First: 2016/08/10].

Chapter, W.J.L., 2019. 3 – FTD spectrum: Neuroimaging across the FTD spectrum. In: Becker, J.T., Cohen, A.D. (Eds.), Progress in Molecular Biology and Translational Science. Academic Press, pp. 187–223.

Seelaar, H., Rohrer, J.D., Pijnenburg, Y.A.L., Fox, N.C., van Swieten, J.C., 2011. Clinical, genetic and pathological heterogeneity of frontotemporal dementia: a review. J. Neurol. Neurosurg. Psychiatry 82 (5), 476–486.

Whitwell, J.L., Xu, J., Mandrekar, J., Boeve, B.F., Knopman, D.S., Parisi, J.E., Senjem, M. L., Dickson, D.W., Petersen, R.C., Rademakers, R., Jack, C.R., Josephs, K.A., 2013. Frontal asymmetry in behavioral variant frontotemporal dementia: clinicoimaging and pathogenetic correlates. Neurobiol. Aging 34 (2), 636–639.

Kril, J.J., Macdonald, V., Patel, S., Png, F., Halliday, G.M., 2005. Distribution of brain atrophy in behavioral variant frontotemporal dementia. J. Neurol. Sci. 232 (1-2), 83–90.

Landin-Romero, R., Kumfor, F., Leyton, C.E., Irish, M., Hodges, J.R., Piguet, O., 2017. Disease-specific patterns of cortical and subcortical degeneration in a longitudinal study of Alzheimer's disease and behavioural-variant frontotemporal dementia. Neuroimage 151, 72–80.

Canu, E., Agosta, F., Mandic-Stojmenovic, G., Stojković, T., Stefanova, E., Inuggi, A., Imperiale, F., Copetti, M., Kostic, V.S., Filippi, M., 2017. Multiparametric MRI to distinguish early onset Alzheimer's disease and behavioural variant of frontotemporal dementia. Neuroimage Clin. 15, 428–438.

Möller, C., Pijnenburg, Y.A.L., van der Flier, W.M., Versteeg, A., Tijms, B., de Munck, J. C., Hafkemeijer, A., Rombouts, S.A.R.B., van der Grond, J., van Swieten, J., Dopper, E., Scheltens, P., Barkhof, F., Vrenken, H., Wink, A.M., 2016. Alzheimer disease and behavioral variant frontotemporal dementia: automatic classification based on cortical atrophy for single-subject diagnosis. Radiology 279 (3), 838–848.

Bruun, M., Koikkalainen, J., Rhodius-Meester, H.F.M., Baroni, M., Gjerum, L.e., van Gils, M., Soininen, H., Remes, A.M., Hartikainen, P., Waldemar, G., Mecocci, P., Barkhof, F., Pijnenburg, Y., van der Flier, W.M., Hasselbalch, S.G., Lötjönen, J., Frederiksen, K.S., 2019. Detecting frontotemporal dementia syndromes using MRI biomarkers. Neuroimage Clin 22, 101711.

Bouts, M.J.R.J., Möller, C., Hafkemeijer, A., van Swieten, J.C., Dopper, E., van der Flier, W.M., Vrenken, H., Wink, A.M., Pijnenburg, Y.A.L., Scheltens, P., Barkhof, F., Schouten, T.M., de Vos, F., Feis, R.A., van der Grond, J., de Rooij, M., Rombouts, S.A. R.B., Zhang, Y.u., 2018. Single subject classification of Alzheimer's disease and behavioral variant frontotemporal dementia using anatomical, diffusion tensor, and resting-state functional magnetic resonance imaging. J. Alzheimers Dis. 62 (4), 1827–1839.

Zhutovsky, P., Vijverberg, E.G.B., Bruin, W.B., Thomas, R.M., Wattjes, M.P., Pijnenburg, Y.A.L., van Wingen, G.A., Dols, A., Solje, E., 2019. Individual prediction of behavioral variant frontotemporal dementia development using multivariate pattern analysis of magnetic resonance imaging data. J. Alzheimers Dis. 68 (3), 1229–1241.

Manera, A.L., Dadar, M., Van Swieten, J.C., Borroni, B., Sanchez-Valle, R., Moreno, F., Laforce Jr, R., Graff, C., Synofzik, M., Galimberti, D., Rowe, J.B., Masellis, M., Tartaglia, M.C., Finger, E., Vandenberghe, R., de Mendonca, A., Tagliavini, F., Santana, I., Butler, C.R., Gerhard, A., Danek, A., Levin, J., Otto, M., Frisoni, G., Ghidoni, R., Sorbi, S., Rohrer, J.D., Ducharme, S., Collins, D.L., 2021. MRI data-driven algorithm for the diagnosis of behavioural variant frontotemporal dementia. J. Neurol. Neurosurg. Psychiatry 92 (6), 608–616.

Zeighami, Y., Ulla, M., Iturria-Medina, Y., et al., Network structure of brain atrophy in de novo Parkinson's disease. Elife 2015;4 doi: 10.7554/eLife.08440 [published Online First: 2015/09/08].

Boucetta, S., Salimi, A., Dadar, M., Jones, B.E., Collins, D.L., Dang-Vu, T.T., 2016. Structural brain alterations associated with rapid eye movement sleep behavior disorder in Parkinson's disease. Sci. Rep. 6 (1).

Dadar, M., Fonov, V.S., Collins, D.L., et al., 2018. A comparison of publicly available linear MRI stereotaxic registration techniques. Neuroimage 174, 191–200. https://doi.org/10.1016/j.neuroimage.2018.03.025 [published Online First: 2018/03/20].